Toughening in electrospun fibrous scaffolds

C. T. Koh and M. L. Oyen

Articles you may be interested in

The effect of shock-wave profile on dynamic brittle failure
J. Appl. Phys. **113**, 103506 (2013); 10.1063/1.4794002

ContinuousDiscontinuous Model for Ductile Fracture
AIP Conf. Proc. **1252**, 245 (2010); 10.1063/1.3457558

A parameter study of separation modes of adhering microcontacts
J. Appl. Phys. **103**, 064902 (2008); 10.1063/1.2874434

Numerical simulation of burst defects in cold extrusion process
AIP Conf. Proc. **908**, 1395 (2007); 10.1063/1.2741004

Measurement of the state of stress in silicon with micro-Raman spectroscopy
J. Appl. Phys. **96**, 7195 (2004); 10.1063/1.1808244

Toughening in electrospun fibrous scaffolds

C. T. Koh[1,2] and M. L. Oyen[1,a]

[1]*Cambridge University Engineering Department, Trumpington Street, Cambridge CB2 1PZ, United Kingdom*
[2]*Faculty of Mechanical and Manufacturing Engineering, Universiti Tun Hussein Onn Malaysia, Parit Raja, 81310 Johor, Malaysia*

Electrospun scaffolds mimic the microstructure of structural collagenous tissues and have been widely used in tissue engineering applications. Both brittle cracking and ductile failure have been observed in scaffolds with similarly random fibrous morphology. Finite element analysis can be used to qualitatively examine the mechanics of these differing failure mechanisms. The finite element modeling demonstrates that the noncontinuum deformation of the network structure results in fiber bundle formation and material toughening. Such toughening is accommodated by varying fiber properties, including allowing large failure strains and progressive damage of the fibers. © 2014 Author(s). All article content, except where otherwise noted, is licensed under a Creative Commons Attribution 3.0 Unported License. [http://dx.doi.org/10.1063/1.4901450]

Scaffolds produced by an electrospinning technique consist of fibrous mats with fiber diameters on the order of nano- to micrometers. These structures resemble the collagen fiber networks found in cartilage, amniotic membranes, cornea, and blood vessels.[1–3] These electrospun scaffolds have been extensively studied in tissue engineering which has great potential in offering solution for damage tissues caused by sports injuries, such as ligament or cartilage rupture, aortic rupture in aneurism, and fetal membrane rupture in premature birth. Tissue regeneration has been improved by applying chemical and mechanical forces on electrospun scaffolds using bioreactors.[4] Such external loading can induce failure, and in this regard, understanding the toughness of electrospun scaffolds becomes critical.

A limitation in electrospun scaffold use is its incompletely understood mechanical performance.[5–7] For instance, gelatin electrospun scaffolds exhibit brittle failure while Polycaprolactone (PCL) electrospun scaffolds exhibited ductile failure, despite the fact that both scaffolds were produced by the same technique and both have similar structural morphology as random networks.[8] The *in situ* fracture testing by scanning electron microscopy (SEM) shows that the formation of fiber bundles through network rearrangement is a key toughening mechanism, but such understanding is not sufficient for the design of biomimetic materials. In particular, the design of electrospun scaffolds, which has many microstructural variables such as network density, fiber diameter, and properties,[7,9–11] requires the understanding of how these material parameters affect their failure mechanisms. However, such understanding remains a challenge due to two main reasons. First, electrospun scaffolds exhibit nonlinear deformation behavior which results from either the longitude stiffening behavior of fibers themselves[12] or from the nonaffine rearrangement of fibrous networks.[13] Such nonlinear deformation responses complicate the network fracture problem because the existing theories used for linear materials are no longer applicable for fibrous materials. Second, fibers have been observed to individually rupture during failure. Previous study focused on studying the critical notch tip opening of fibrous networks prior to crack propagation.[14,15] The failure

---

[a]Author to whom correspondence should be addressed. Electronic mail: mlo29@cam.ac.uk. Telephone: +44 1223 332 680. Fax: +44 1223 332662.

3, 014908-1

criterion was defined by the tensile strength of a fiber. Such studies have not considered either the nonlinear behavior or the rupture of fibers found during failure mechanisms.

The objective of the work presented here is to explore crack propagation in fibrous networks at and near the crack tip not only for the particular case of electrospun scaffolds but also for the more general case of fibrous materials with diameters of nano- to micrometers. There is no existing analytical solution to this problem, therefore necessitating the use of the finite element (FE) method to reveal the physics and its dependence on fiber properties and fiber diameter. Previous laboratory observations, including brittle cracking and fiber bundle formation,[8] were simulated using an element elimination technique allowing for active crack propagation.

The modeled two-dimensional domain consisted of a 50×75 μm fibrous network with a 12.5 μm notch length. The fibrous networks were generated in MATLAB (The MatWorks, Natick, MA) by constructing lines from random points with random angles. The network was modelled as partially cross-linked with network branching angles of 30°, only when the intersection angle between two fibers was less than this prescribed branch angle was a cross-link introduced. For all other intersection points, the fibrils were allowed to slide friction-free along each other. The fibers were then meshed with length equal or smaller than 1 μm, before being imported to, and modeled by beam elements in FE software ABAQUS (Version 6.7, SIMULIA, Providence, RI). All simulations were performed using nonlinear FE analysis which considers large strain and rotation.

The outer boundary was subjected to the displacement field associated with the macroscopic crack tip field for a homogenous and isotropic solid; by defining the origin at the notch root, the displacement components (u_1, u_2) can be expressed in terms of the polar co-ordinates (r, θ) as[16]

$$u_1 = \frac{1}{2}\sqrt{\frac{r}{2\pi}}\frac{K_I}{G}\left(\kappa + 1 + 2\cos^2\frac{\theta}{2}\right)\sin\frac{\theta}{2}, \tag{1}$$

$$u_2 = \frac{1}{2}\sqrt{\frac{r}{2\pi}}\frac{K_I}{G}\left(-\kappa + 1 + 2\sin^2\frac{\theta}{2}\right)\cos\frac{\theta}{2}. \tag{2}$$

The origin for the K-dominant expression (Eqs. (1) and (2)) is located at the crack tip. The model assumes the expression origin stays at the same location throughout the simulation, despite the fact that the crack propagation results in a moving crack tip.

The effect of both nonlinear and progressive damages of individual fibers on the network fracture was investigated. Fiber property profiles were studied as shown in Figure 1(b); a fiber was assigned a Young's modulus of 470 MPa, a plastic modulus of 346 MPa, and a yield strain of 33%; the progressive damage is then modeled by a negative stress-strain slope of 490 MPa. Four failure criteria were defined as follows: brittle and elastic fibers failed at $\varepsilon_f = 0.12$ (point P1) and $\varepsilon_f = 0.35$
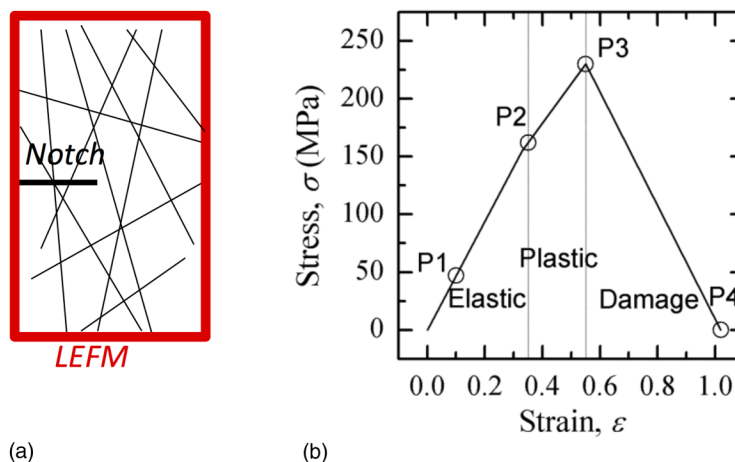

FIG. 1. (a) Schematic illustration of FE models consisting of fibrous networks with a notch and Linear Elastic Fracture Mechanics (LEFM) boundary condition. (b) The fiber properties assigned in FE models consisting four failure points (P1, P2, P3, and P4). The fiber profile considers elastic, plastic, and progressive damage behaviors.
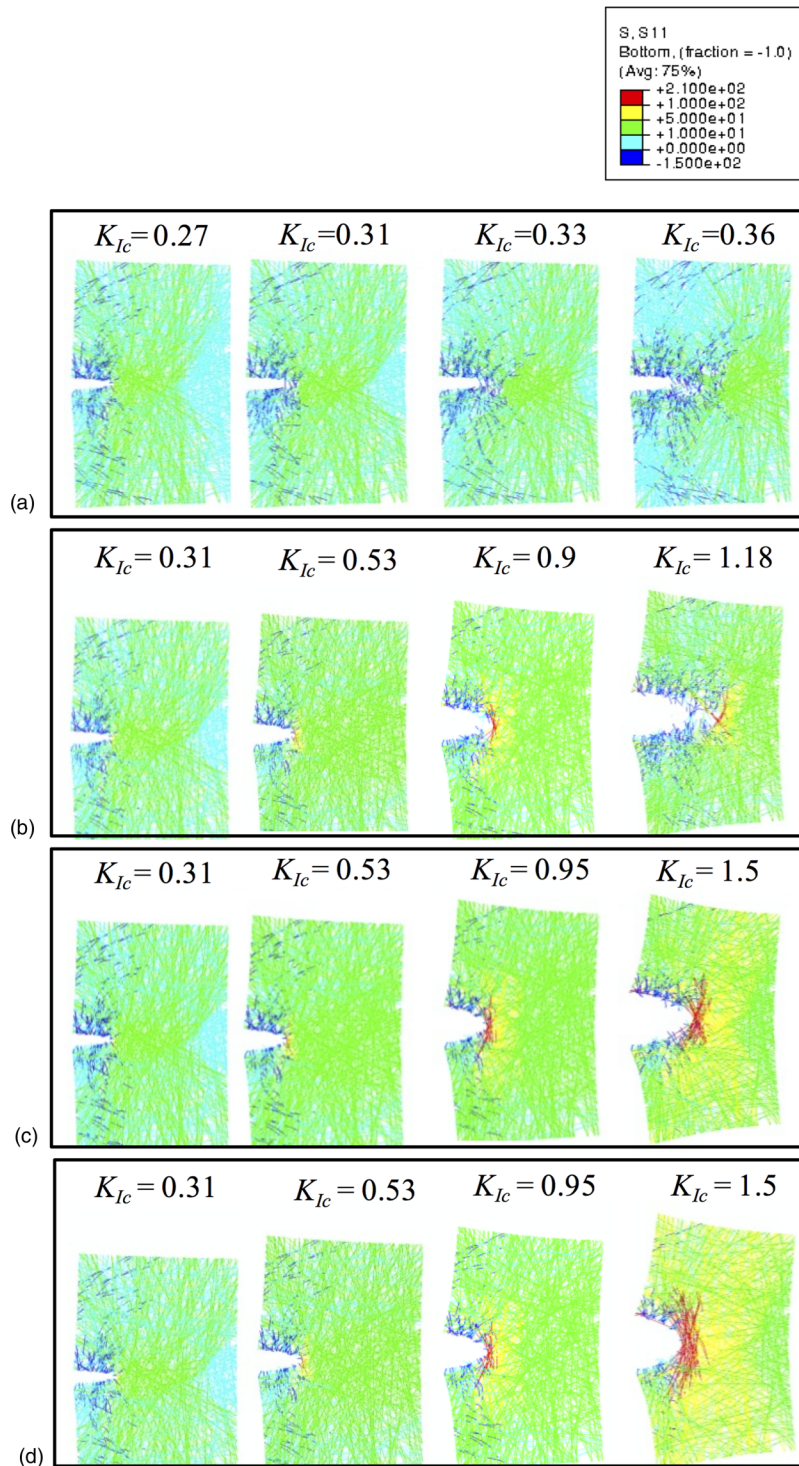
FIG. 2. The influence of fiber properties on the failure mechanisms of fibrous networks. Four fiber properties studied here were P1 (a), P2 (b), P3 (c), and P4 (d). The deformed networks were shown corresponding to the stress intensity factor K_{Ic} (units of $MPa\sqrt{m}$) used to assign the displacement on their boundaries.

(point P2), ductile and elastic-plastic fibers failed at $\varepsilon_f = 0.57$ (point P3) and at $\varepsilon_f = 1.02$ (point P4). Note that only the P4 case considers the progressive damage. The fibers were simulated to be ruptured once they reach the failure criterion. These ruptured fibers were then removed using an element elimination technique in the FE analysis.

Figure 2 shows the comparison of crack propagation evaluation among three identical networks assigned with different failure strains. The evolution of crack propagation here was described by stress intensity factor K, which corresponds to the K-dominant strain field assigned at the boundaries. The larger the stress intensity factor, the larger the strain applied at the boundaries of the fibrous networks. The fracture of the network was governed by the failure strain of fibers. The crack in the network with the smallest failure strain (failure point P1) started to propagate at small stress intensity factor $K_{Ic} = 0.31\ MPa\sqrt{m}$ (Figure 2(a)). The corresponding notch opening remained small; a significant stress concentration occurred at the crack tip and the nonlinear region involving network deformation was confined to a small region in the vicinity of the crack tip. Compared to this weakest fibrous network, the network with an increased failure strain (failure point P2) showed larger and blunted crack openings without crack propagation at $K_{Ic} = 0.31\ MPa\sqrt{m}$ (Figure 2(b)). The nonlinear region ahead of the notch tip was also expanded by having more fibers aligned perpendicular to the crack tip and the crack only started to propagate at $K_{Ic} = 0.53\ MPa\sqrt{m}$. A similar trend occurred for the network with the largest failure strain (failure point P3). The increased failure strain and plastic deformation postponed the crack propagation at $K_{Ic} = 0.95\ MPa\sqrt{m}$, by allowing more fiber realignment to form a large blunted crack (Figure 2(c)). This allowed the stress to be distributed and energy dissipated ahead of the crack tip.

The consideration of progressive damage in fibers allowed for fiber bundles to be formed ahead of notch tip (Figure 2(d)). Unlike with brittle fibers, the progressive damage within the fibers allowed fibers to realign and this was what formed fiber bundles aligned transverse to the crack propagation direction. The fiber bundles withstood large stress in front of the crack tip without fiber rupture at $K_{Ic} = 1.5\ MPa\sqrt{m}$. This progressive damage is likely to occur in nature, particularly for those materials which have hierarchical structure within a fiber;[17–19] by having a hierarchical structure, the fiber does not break abruptly, but will rupture in a progressive manner. The reduced stiffness remaining in the fibers prevented excess stress from being applied to other undamaged fibers. The post damage deformation is also likely to occur in materials such as PCL and collagen
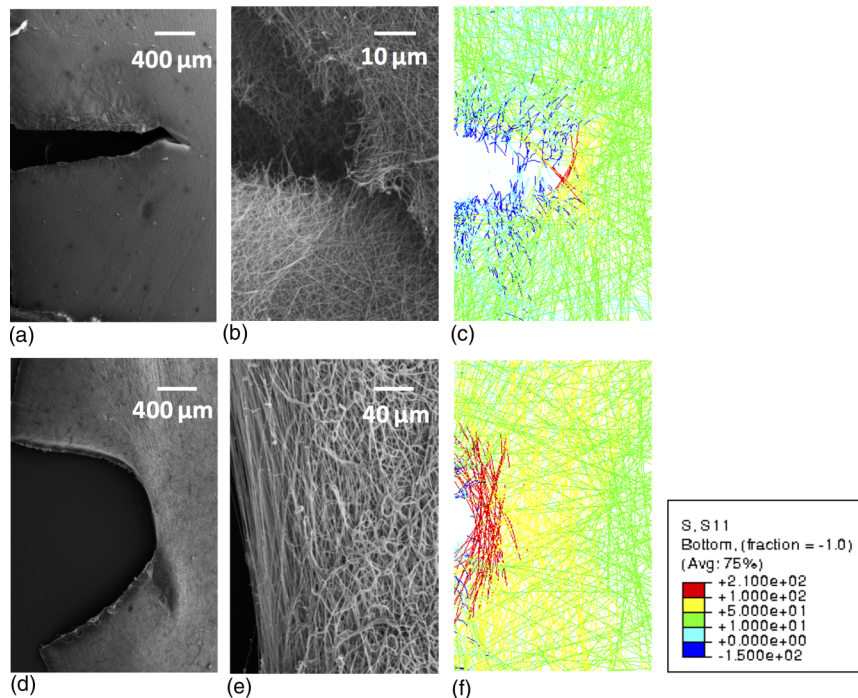

FIG. 3. SEM images of brittle failure in the vicinity of notch root in gelatine fibrous network ((a) and (b)) as compared to the FE results simulated by P2 model (c), and ductile failure in the vicinity of notch root in PCL fibrous network ((d) and (e)) as compared to the FE results simulated by P4 model (f).

fibers. These fibers do not break immediately after reaching the material strength. Rather, their stress is reduced allowing them to elongate for a large strain before rupture.

While the fiber properties are important, the presence of microscopic network structure is relatively important to allow for the mechanisms of fiber rearrangement and reorientation. The presence of network structure resulted in an extreme defect tolerant characteristic and allowed the microstructures to deform in a noncontinuum manner. Such noncontinuum deformation was observed in fiber bundles formed ahead of the crack tip (Figures 2(c) and 2(d)). A non-compatible strain field was observed in the fibrous networks; the partial bonding allowed the neighboring fibers to move with gaps or overlaps. Fibers aligned perpendicularly to the notch tip had a large tensile stress while those aligned parallel to the crack tip had small or even minute compressive stress.

For comparison, both brittle cracking in gelatin electrospun scaffolds and ductile toughening in PCL electrospun scaffolds are shown in Figure 3. Both scaffolds were produced by the same sample preparation procedure used in the previous study.[8] The deformation of their microscopic networks around the crack tips was also visualized in a FEI Philips (UK) XL30 field emission gun scanning electron microscope equipped with an Oxford Instruments (UK) INCA EDX system. The experiment observation agrees well with the numerical results, therefore providing a validation of the FE analysis in capturing failure mechanisms. For brittle cracking, random network morphology around the crack tip was observed in experiments and numerical results. For ductile failure, fiber bundles were formed across the region in front of the notch tip for both results.

The FE method transcends the limitations of continuum mechanics, by simulating the noncontinuum deformation of fibrous networks around the crack tips. Such noncontinuum deformation in fibrous networks allows for the formation of fiber bundles, which toughens the networks. In addition to the existence of random network structure, the fiber bundles will only form with the accommodation of specific fiber characteristics including large failure strain and progressive damage behavior of fibers. Such understanding suggests design principles in the production of electrospun scaffolds with improved toughness.

[1] P. Fratzl, *Collagen Structure and Mechanics* (Springer Science+Bussiness Media, 2008).

[2] S. E. Calvin and M. L. Oyen, "Microstructure and mechanics of the chorioamnion membrane with an emphasis on fracture properties," Ann. N. Y. Acad. Sci. **1101**, 166–85 (2007).

[3] M. L. Oyen, R. F. Cook, T. Stylianopoulos, V. H. Barocas, S. E. Calvin, and D. V. Landers, "Uniaxial and biaxial mechanical behavior of human amnion," J. Mater. Res. **20**(11), 2902–2909 (2005).

[4] J. A. Burdick and G. D. Prestwich, "Hyaluronic acid hydrogels for biomedical applications," Adv. Mater. **23**(12), H41–H56 (2011).

[5] K. Tonsomboon, C. T. Koh, and M. L. Oyen, "Time-dependent fracture toughness of cornea," J. Mech. Behav. Biomed. Mater. **34**, 116–123 (2014).

[6] U. Stachewicz, I. Peker, W. Tu, and A. H. Barber, "Stress delocalization in crack tolerant electrospun nanofiber networks," ACS Appl. Mater. Interfaces **3**(6), 1991–1996 (2011).

[7] D. Papkov, Y. Zou, M. N. Andalib, A. Goponenko, S. Z. D. Cheng, and Y. A. Dzenis, "Simultaneously strong and tough ultrafine continuous nanofibers," ACS Nano. **7**(4), 3324–3331 (2013).

[8] C. T. Koh, D. G. T. Strange, K. Tonsomboon, and M. L. Oyen, "Failure mechanisms in fibrous scaffolds," Acta Biomater. **9**(7), 7326–7334 (2013).

[9] Z. Huang, Y. Zhang, M. Kotaki, and S. Ramakrishna, "A review on polymer nanofibers by electrospinning and their applications in nanocomposites," Compos. Sci. Technol. **63**, 2223–2253 (2003).

[10] A. Cipitria, A. Skelton, T. R. Dargaville, P. D. Dalton, and D. W. Hutmacher, "Design, fabrication and characterization of PCL electrospun scaffolds," J. Mater. Chem. **21**(26), 9419 (2011).

[11] K. Tonsomboon and M. L. Oyen, "Composite electrospun gelatin fiber-alginate gel scaffolds for mechanically robust tissue engineered cornea," J. Mech. Behav. Biomed. Mater. **21**, 185–194 (2013).

[12] C. Storm, J. J. Pastore, F. C. MacKintosh, T. C. Lubensky, and P. A. Janmey, "Nonlinear elasticity in biological gels," Nature **435**, 191–194 (2005).

[13] P. R. Onck, T. Koeman, T. Dillen, and E. Giessen, "Alternative explanation of stiffening in cross-linked semiflexible networks," Phys. Rev. Lett. **95**, 178102 (2005).

[14] C. T. Koh and M. L. Oyen, "Branching toughens fibrous networks," J. Mech. Behav. Biomed. Mater. **12**, 74–82 (2012).

[15] C. T. Koh and M. L. Oyen, "Fracture toughness of fibrous membranes," Technische Mechanik **32**(2–5), 333–341 (2012).

[16] M. F. Kanninen and C. H. Popelar, *Advanced Fracture Mechanics* (Oxford University Press, 1985), p. 145.

[17] *Orthopaedic Basic Science*, edited by S. R. Simon (American Academy of Orthopaedic Surgeons, 1994).

[18] P. Fratzl and R. Weinkamer, "Nature's hierarchical materials," Prog. Mater. Sci. **52**(8), 1263–1334 (2007).

[19] J. Kastelic, A. Galeski, and E. Baer, "The multicomposite structure of tendon," Connect. Tissue Res. **6**, 11–23 (1978).